Cell Reports, Volume *42*

Supplemental information

Cell-type-specific disruption of cortico-striatal circuitry drives repetitive patterns of behavior in fragile X syndrome model mice

Francesco Longo, Sameer Aryal, Paul G. Anastasiades, Marta Maltese, Corey Baimel, Federica Albanese, Joanna Tabor, Jeffrey D. Zhu, Mauricio M. Oliveira, Denise Gastaldo, Claudia Bagni, Emanuela Santini, Nicolas X. Tritsch, Adam G. Carter, and Eric Klann

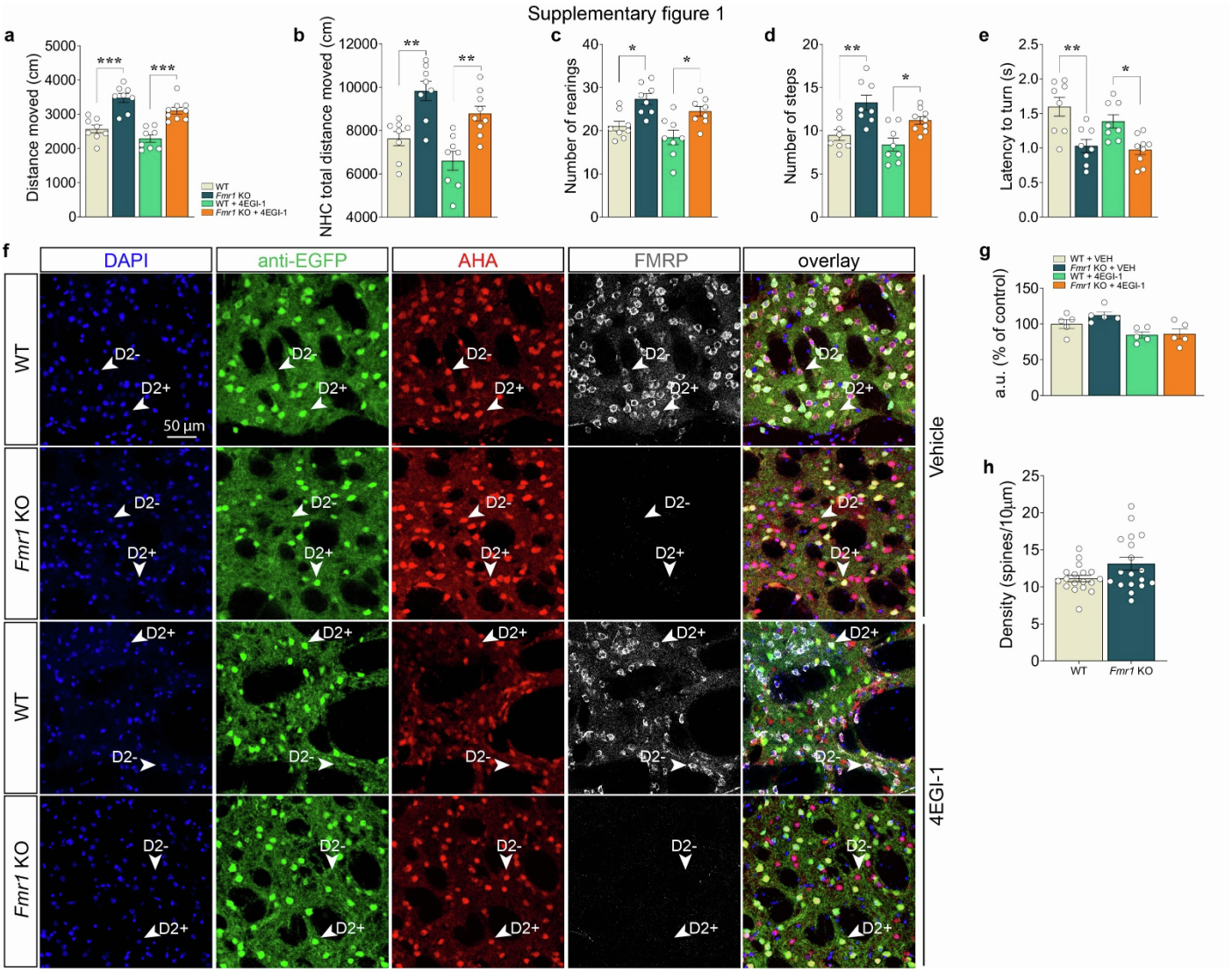

Figure S1. 4EGI-1 does not correct increased locomotor activity in *Fmr1* KO mice. Lack of *Fmr1* does not results in dysregulated *de novo* translation in Drd2-SPNs and does not alter overall dendritic spine density in the DLS.

Fmr1 KO mice show no change in general locomotor activity compared to WT control mice after ICV injection of 4EGI-1 (**a-e**). **a**, Summary plot of spontaneous locomotor activity expressed as distance moved (cm) during the open field test over 15 min in *Fmr1* KO and WT mice treated with either 4EGI-1 or VEH (two-way ANOVA followed by Bonferroni's post-hoc test was conducted; genotype x treatment interaction: $F_{(1,29)}$= 0.16, P=0.69; genotype: $F_{(1,29)}$= 58.08, ***P<0.001; treatment: $F_{(1,29)}$= 8.29, **P<0.01; n=8-9 mice/genotype/treatment). **b**, Summary plot of the novelty-induced locomotor activity expressed as a novel home cage (NHC) distance moved (cm) in a 60 minutes test during novel home cage test in *Fmr1* KO and WT mice treated with either 4EGI-1 or VEH (two-way ANOVA followed by Bonferroni's post-hoc test was conducted; genotype x treatment interaction: $F_{(1,29)}$= 0.00076, P=0.97; genotype: $F_{(1,29)}$= 31.24, ***P<0.001; treatment: $F_{(1,29)}$= 7.02, *P<0.05; n=8-9 mice/genotype/treatment). **c**, Summary plot of vertical activity expressed as number of rearing episodes (number of counts) during the cylinder test over 5 min in *Fmr1* KO and WT mice treated with either 4EGI-1 or VEH (two-way ANOVA followed by Bonferroni's post-hoc test was conducted; genotype x treatment interaction: $F_{(1,28)}$= 0.0063, P=0.93; genotype: $F_{(1,28)}$= 22.08, ***P<0.001; treatment: $F_{(1,28)}$= 4.32, *P<0.05; n=8 mice/genotype/treatment). **d**, Summary plot of average number of steps during drag in *Fmr1* KO and WT mice treated with either 4EGI-1 or VEH (two-way ANOVA followed by Bonferroni's post-hoc test was conducted; genotype x treatment interaction: $F_{(1,29)}$= 0.51, P=0.48; genotype: $F_{(1,29)}$= 23.47, ***P<0.001; treatment: $F_{(1,29)}$= 5.37, *P<0.05; n=8-9 mice/genotype/treatment). **e**, Summary plot of latency to turn (s) during pole test in *Fmr1* KO and WT mice treated with either 4EGI-1 or VEH (two-way ANOVA followed by Bonferroni's post-hoc test was conducted; genotype x treatment interaction: $F_{(1,29)}$= 0.61, P=0.44; genotype: $F_{(1,29)}$= 23.59, ***P<0.001; treatment: $F_{(1,29)}$= 1.77, P=0.19; n=8-9 mice/genotype/treatment). All data are shown as mean ± s.e.m.; *P< 0.05, **P< 0.01, ***P< 0.001 *Fmr1* KO versus WT mice. **f**, Representative DLS immunofluorescence images of DAPI (blue), anti-EGFP (green), anti-FMRP (grey) and incorporation of AHA

(red) detected by FUNCAT with alkyne-Alexa 647 in cortico-striatal slices from *Fmr1* KO/Drd2 EGFP BAC transgenic mice and their WT littermates (scale bar represents 50 µm) treated with VEH (first two rows from the top) or 4EGI-1(last two rows from the top). **g**, Quantification of increased AHA-alkyne-Alexa 647 signal in fluorescent arbitrary units (a.u.) expressed as % of control in Drd2-SPNs (anti-EGFP+ neurons; green) from DLS *Fmr1* KO/Drd2 EGFP BAC transgenic mice and their WT littermates. Cell soma intensity was measured in ImageJ software (FIJI). Statistical significance was determined by using two-way ANOVA followed by Bonferroni's multiple comparisons test (genotype x treatment interaction: $F_{(1,16)}$= 0.85, P=0.37; genotype: $F_{(1,16)}$= 1.42, P=0.25; treatment: $F_{(1,16)}$= 12.79, $^{**}P$<0.01). Data are shown as mean ± s.e.m. of n = 5/6 mice per group (average of n = 20 somas per slice, n = 2 slices per mouse, from three independent experiments). **h**, *Fmr1* KO mice show no significant difference in overall dendritic spine density in DLS (Mann-Whitney test, P=0.181).

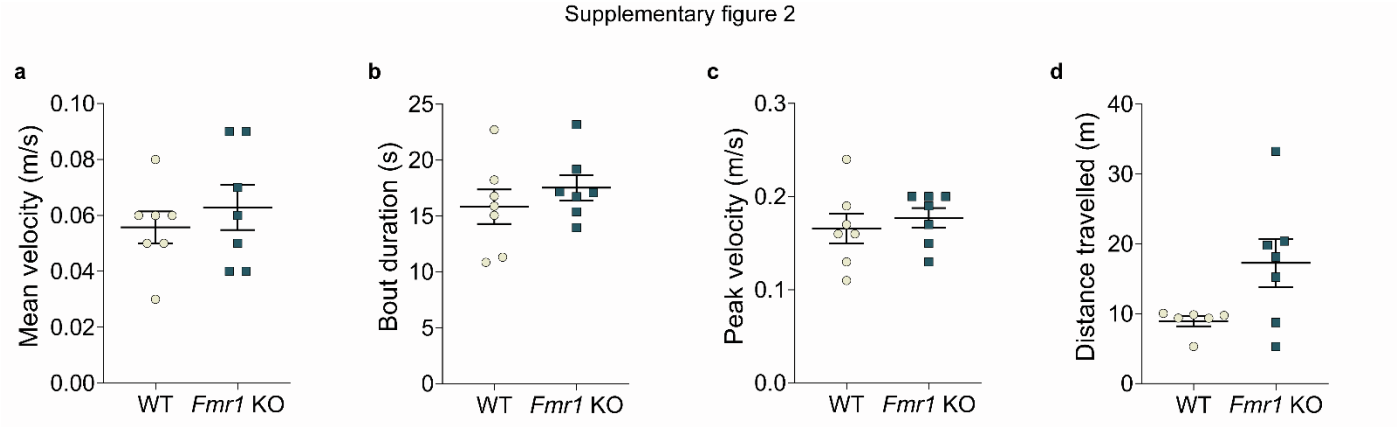

Figure S2. Self-initiated forward locomotion was comparable between WT and *Fmr1* KO mice.

Self-initiated forward locomotion on treadmill during *in vivo* two-photon imaging. **a**, Summary plot of mean self-initiated treadmill velocity in WT (n= 4) or *Fmr1* KO (n= 4) mice (P = 0.63; Mann-Whitney test, n=7 imaging sessions per genotype). **b**, Same as (a) for locomotor bout duration (P= 0.38; Mann-Whitney test, n=7 imaging sessions per genotype). **c**, Same as (a) for locomotor peak velocity (P = 0.40; Mann-Whitney test, n=7 imaging sessions per genotype). **d**, Same as (a) for total distance travelled (P = 0.051; Mann-Whitney test, n=6-7 per genotype).

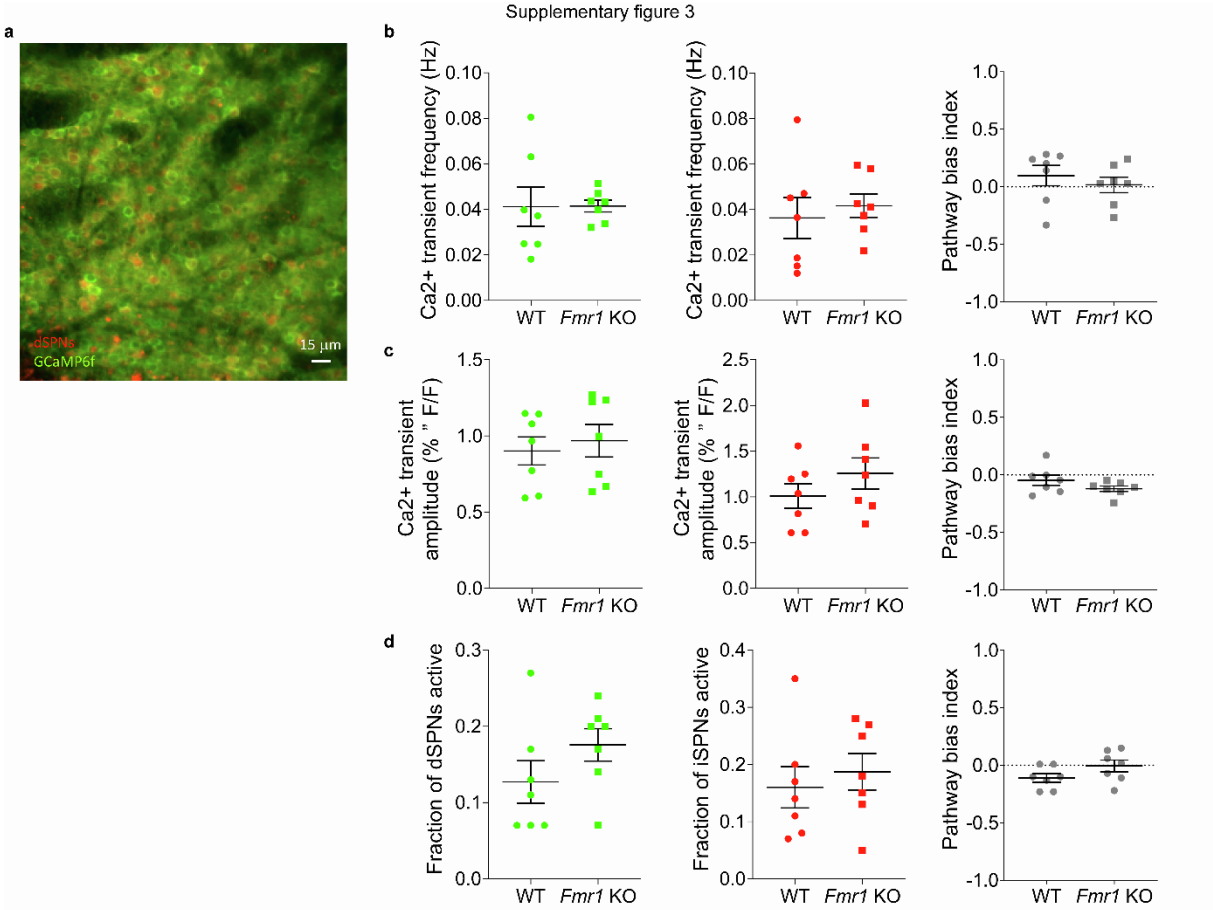

Figure S3. The mean amplitude, frequency of Ca^{2+} transients imaged per active dSPN and iSPN, and the total fraction of all imaged dSPNs and iSPNs recruited during self-initiated forward locomotion was comparable between genotypes.

a, Representative two-photon maximum projection image of dorsal striatum. Red: tdTomato-labeled dSPNs; green: striatal neurons expressing GCaMP6f (scale bar: 15 µm). **b**, Mean Ca^{2+} transient frequency per dSPN (left, green) and iSPN (middle, red) active during self-initiated movement in each of 7 FOVs from 4 mice per genotype. Right: mean Ca^{2+} transient frequency bias index (Frequency: dSPN, $P = 0.53$; iSPNs, $P = 0.53$; pathway bias index, $P = 0.32$; Mann-Whitney test, n = 7 fields of view (FOVs) per genotype). **c**, Same as (b) for mean amplitude of Ca^{2+} transients in active dSPNs and iSPNs (Amplitude: dSPN, $P = 0.46$; iSPNs, $P = 0.38$; pathway bias index, $P = 0.21$; Mann-Whitney test, n = 7 FOVs per genotype). **d**, Same as (b) for the total fraction of all imaged dSPNs or iSPNs that exhibit Ca^{2+} transients (dSPN, $P = 0.15$; iSPNs, $P = 0.53$; pathway bias index, $P = 0.09$; Mann-Whitney test, n = 7 FOVs per genotype).

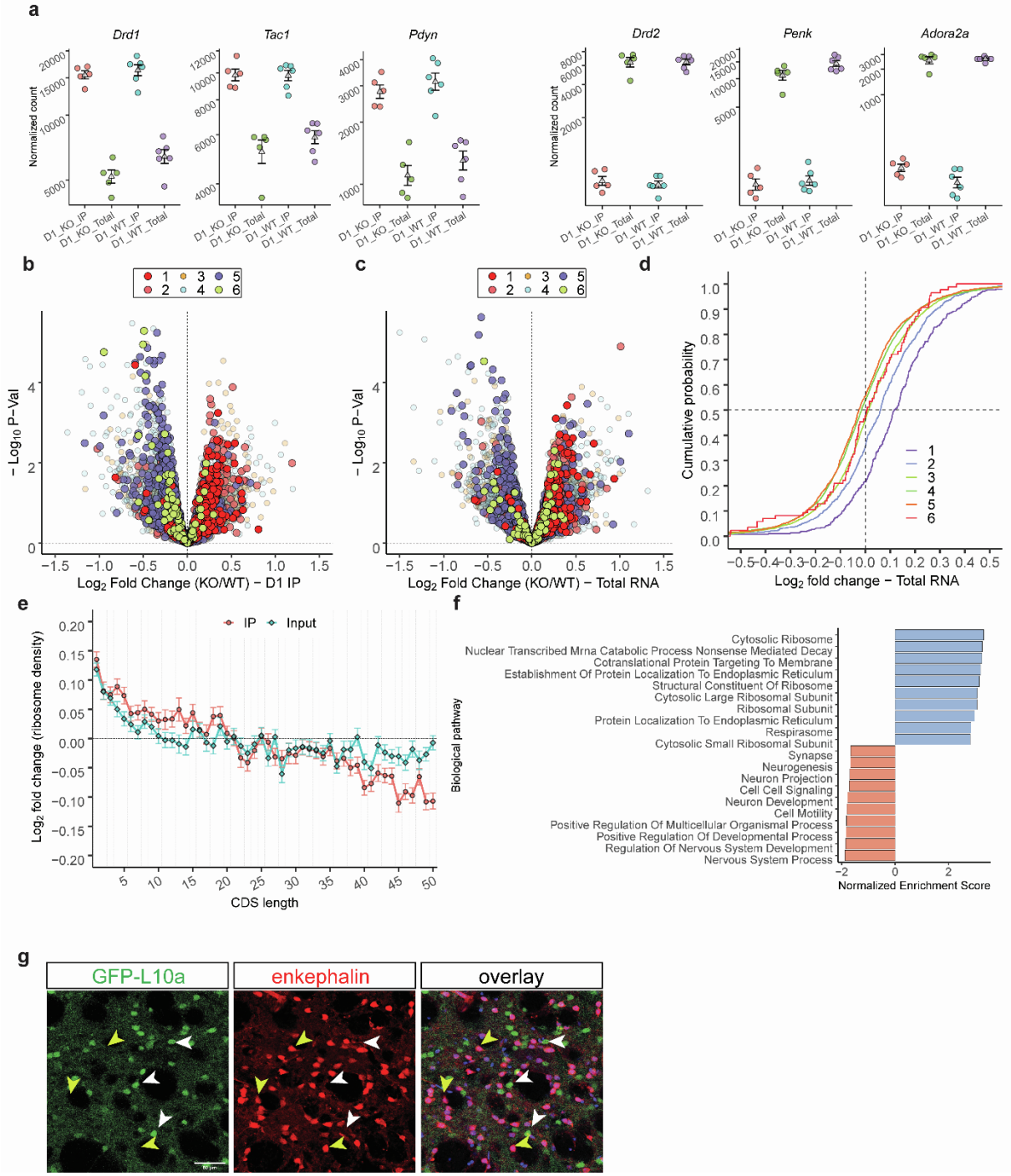

Figure S4. Drd1-TRAP enriches for Drd1 marker genes and Drd1-SPNs show selective expression of GFP-L10a.

a, Trap-Seq of Drd1-SPNs reveals an enrichment of D1 markers and re- duction of markers of Drd2-SPNs. Characteristic markers of Drd1-SPNs including dopamine receptor D1 (Drd1), substance P (Tac1), and dynorphin (Pdyn) are enriched in the IP, while dopamine receptor D2 (Drd2), adenosine 2a receptor (Adora2a), and enkephalin (Penk), which are characteristic markers of D2 MSNs, are reduced relative to their overall mRNA expression in the striatum, in both WT and FXS mice. **b**, Significance (unadjusted (nominal) p-value) vs. log2-fold-change in ribosome association (IP) in Drd1-SPNs and **c**, overall striatal mRNA expression (Total) between FXS and WT mice. Messenger RNAs are divided into six bins in ascending order of their CDS lengths, with bin 1 harboring mRNAs with the shortest CDSs, and bin 6 the longest. mRNAs are color-coded by their CDS length bins. mRNAs with long CDSs are enriched in genes showing significant reduction in ribosome association in D1 MSNs of mice lacking FMRP, while those with the shortest CDSs are over-represented in

genes exhibiting significant increase in ribosome association. A similar but weaker trend is also observed in alterations in overall RNA expression in the striata of FXS model mice. **d**, Cumulative distribution of log2-fold-changes (FXS/WT) in RNA expression in the striatum of FXS model mice, as a function of CDS length. mRNAs with the shortest CDSs are especially likely to show elevated expression in the striatum. **e**, Comparison of log2-fold-changes in ribosome association in Drd1-SPNs of FXS, and overall RNA expression in the striatum, by CDS length. mRNAs are divided into 50 bins, with each containing 201 mRNAs. mRNAs with the shortest CDSs exhibit increased ribosome association in D1 neurons of FXS model mice, while those with the longest CDSs exhibit reduced ribosome association. A positive-to-negative gradation is observed with CDS length in log2-fold-changes in ribosome association. LFCs in overall mRNA expression of short CDS mRNAs in the striata of mice lacking FMRP closely track the LFCs in ribosome association in D1 MSNs of FXS model mice. For long CDS mRNAs, much larger and overwhelmingly negative alterations in ribosome association in Drd1-SPNs are observed compared to overall mRNA expression in the striata. **f**, Enrichment scores of the top 10 gene ontologies (GOs) enriched in the WT or FXS striata, determined by GSEA on genes ranked by their fold changes RNA expression. mRNAs coding for ribosomal proteins are overabundant in FXS striata, while GOs associated to synapse and glutamatergic signaling are reduced. **g**, Confocal images show selective expression of GFP-L10a in Drd1-SPNs verified at the protein expression level by immunostaining coronal slices containing the DLS with enkephalin antibody (red), a marker for Drd2-SPNs. EGFP-L10a expression did not co-stained with enkephalin in DLS Drd1-SPNs of Drd1a-bacTRAP transgenic mice (scale bar represents 50 μm). White arrows indicate Drd1-SPNs (green) and enkephalin (red) staining; yellow arrows indicate non-Drd1-SPNs and enkephalin (red) co-staining.

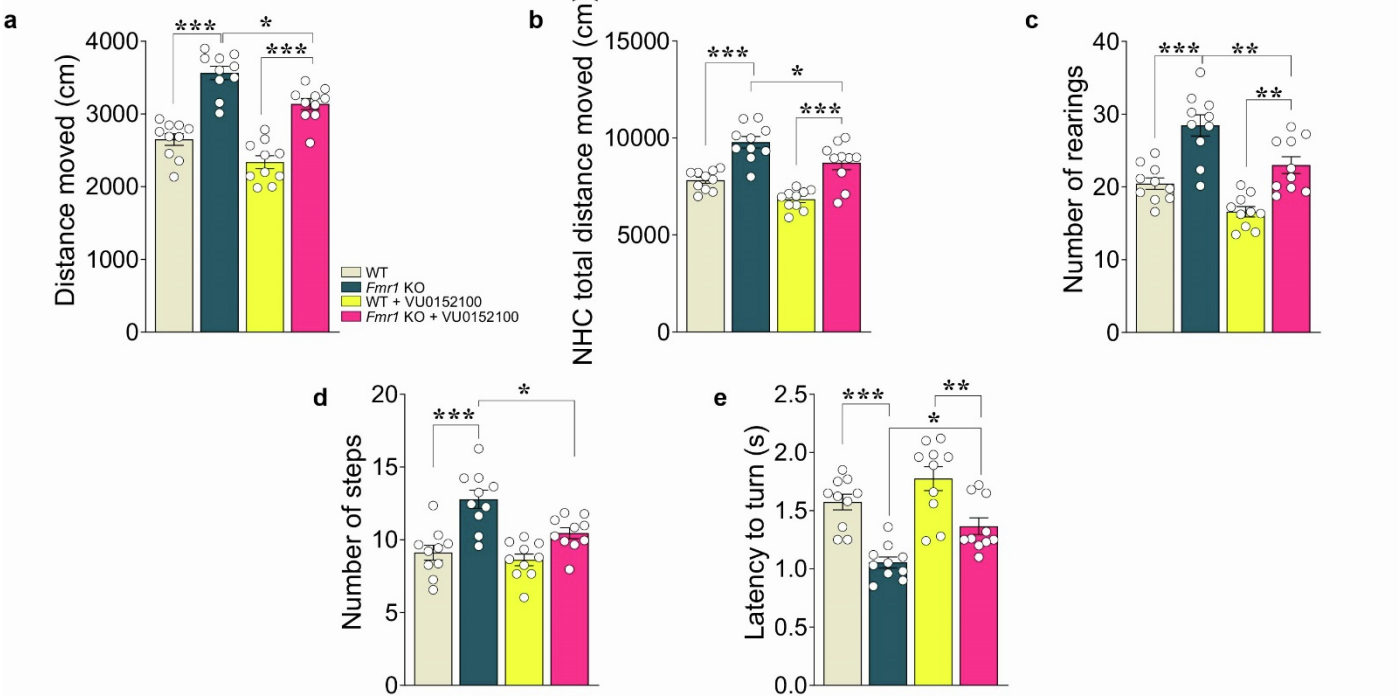

Figure S5. VU0152100 does not correct increased general locomotor in *Fmr1* KO mice.

Fmr1 KO mice show no change in general locomotor activity compared to WT control mice after i.p. injection of M4R PAM VU0152100 (**a-e**). **a**, Summary plot of spontaneous locomotor activity expressed as distance moved (cm) during the open field test over 15 min in *Fmr1* KO and WT mice treated with either VU0152100or VEH (two-way ANOVA followed by Bonferroni's post-hoc test was conducted; genotype x treatment interaction: $F_{(1,36)}$= 0.46, P=0.50; genotype: $F_{(1,36)}$= 103.7, ***P<0.001; treatment: $F_{(1,36)}$= 19.26, ***P<0.001; n=10 mice/genotype/treatment). **b**, Summary plot of the novelty-induced locomotor activity expressed as a novel home cage (NHC) distance moved (cm) in a 60 minutes test during novel home cage test in *Fmr1* KO and WT mice treated with either VU0152100 or VEH (two-way ANOVA followed by Bonferroni's post-hoc test was conducted; genotype x treatment interaction: $F_{(1,36)}$= 0.02, P=0.88; genotype: $F_{(1,36)}$= 59.69, ***P<0.001; treatment: $F_{(1,36)}$= 16.18, ***P<0.001; n=10 mice/genotype/treatment). **c**, Summary plot of vertical activity expressed as number of rearing episodes (number of counts) during the cylinder test over 5 min in *Fmr1* KO and WT mice treated with either VU0152100 or VEH (two-way ANOVA followed by Bonferroni's post-hoc test was conducted; genotype x treatment interaction: $F_{(1,36)}$= 0.56, P=0.46; genotype: $F_{(1,36)}$= 45.25, ***P<0.001; treatment: $F_{(1,36)}$= 19.01, ***P<0.001; n=10 mice/genotype/treatment). **d**, Summary plot of average number of steps during drag in *Fmr1* KO and WT mice treated with either VU0152100 or VEH (two-way ANOVA followed by Bonferroni's post-hoc test was conducted; genotype x treatment interaction: $F_{(1,36)}$= 3.49, P=0.07; genotype: $F_{(1,36)}$= 31.45, ***P<0.001; treatment: $F_{(1,36)}$= 8.27, *P<0.05; n=10 mice/genotype/treatment). **e**, Summary plot of latency to turn (s) during pole test in *Fmr1* KO and WT mice treated with either VU0152100 or VEH (two-way ANOVA followed by Bonferroni's post-hoc test was conducted; genotype x treatment interaction: $F_{(1,36)}$= 0.53, P=0.47; genotype: $F_{(1,36)}$= 38.36, ***P<0.001; treatment: $F_{(1,36)}$= 11.73, *P<0.05; n=10 mice/genotype/treatment). All data are shown as mean ± s.e.m.; *P< 0.05, **P< 0.01, ***P< 0.001 *Fmr1* KO versus WT mice.

Supplementary Figure 6

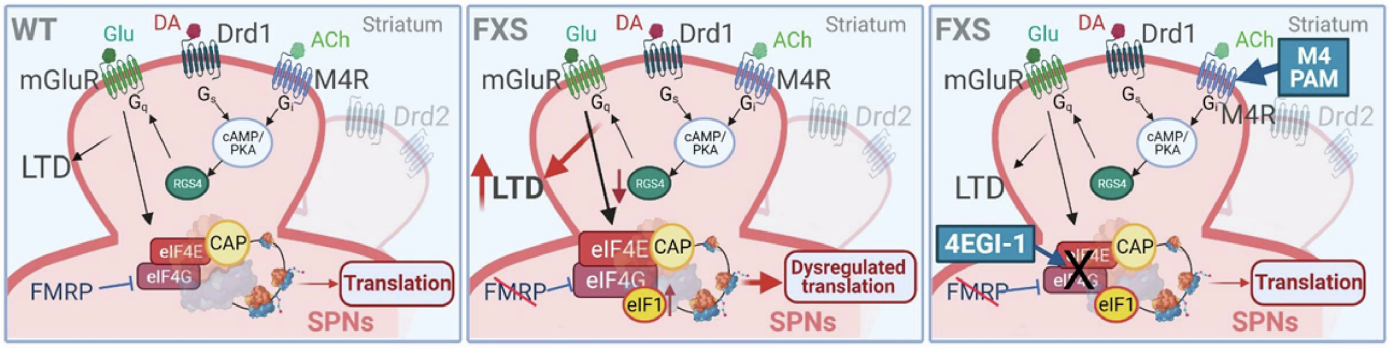

Figure S6. Proposed model for correction of FXS by either 4EGI-1 or M4R PAM VU0152100

Loss of FMRP in FXS leads to enhanced eIF4E-eIF4G interaction resulting in net increase in de novo cap-dependent translation in Drd1-SPNs in *Fmr1* KO mice. In FXS, the absence of FMRP leads to the excessive synthesis of eIF1 and downregulated expression of RGS4 therefore cortico-striatal LTD is enhanced in *Fmr1* KO mice. By using 4EGI-1 or M4R PAM VU0152100 LTD and aberrant behavior are rescued. 4EGI-1 also normalizes protein synthesis rate in the striatum of *Fmr1* KO mice.

Table S1

Main Figures	Test performed	P value	N number
Figure 1a	unpaired *t* test; $t_{(14)}$= 4.06	**P <0.01	n=8 mice/genotype
Figure 1b	unpaired *t* test; $t_{(14)}$= 3.51	**P <0.01	n=8 mice/genotype
Figure 1c	unpaired *t* test; $t_{(14)}$= 3.91	**P <0.01	n=8 mice/genotype
Figure 1d	unpaired *t* test; $t_{(15)}$= 2.70	*P <0.05	n= 8-9 mice/genotype
Figure 1e	unpaired *t* test; $t_{(18)}$= 3.60	**P <0.01	n=10 mice/genotype
Figure 1f	unpaired *t* test; $t_{(19)}$= 4.68	***P <0.001	n= 10-11 mice/genotype
Figure 1g	unpaired *t* test; $t_{(15)}$= 4.99	***P <0.001	n= 8-9 mice/genotype
Figure 1h	unpaired *t* test; $t_{(14)}$= 2.90	*P <0.05	n=8 mice/genotype
Figure 1j	two-way RM ANOVA Bonferroni's multiple comparisons test; time x genotype, $F_{(2,54)}$ = 8.51	P = 0.0006	*n*=12-15 slices from 8 mice/genotype
Figure 2a	two-way ANOVA Bonferroni's multiple comparisons test; genotype x treatment interaction: $F_{(1,20)}$=12.18	P = 0.0023	n= 5-7 independent lysates from 5-7 mice per group
Figure 2a	genotype: $F_{(1, 20)}$ = 2.854	P = 0.1067	
Figure 2a	treatment: $F_{(1, 20)}$= 32.24	P <0.0001	
Figure 2b	two-way ANOVA Bonferroni's multiple comparisons test; genotype x treatment interaction: $F_{(1, 12)}$ = 9.260	P = 0. 0102	n= 4 independent lysates from 4 mice per group
Figure 2b	genotype: $F_{(1, 12)}$ = 16.10	P = 0.0017	
Figure 2b	treatment: $F_{(1, 12)}$ = 0.2815	P = 0.6054	
Figure 2d	two-way RM ANOVA Bonferroni's multiple comparisons test; time x genotype, $F_{(6,136)}$ = 4.672	P = 0.0002	n=18 slices per group from 9 mice/genotype
Figure 2f	two-way ANOVA Bonferroni's multiple comparisons test; genotype x treatment interaction: $F_{(1, 28)}$ = 7.45	*P <0.05	n=8 mice/genotype/treatment
Figure 2f	genotype: $F_{(1, 28)}$ = 9.61	**P <0.01	
Figure 2f	treatment: $F_{(1, 28)}$ = 5.57	*P <0.05	
Figure 2g	two-way ANOVA Bonferroni's multiple comparisons test; genotype x treatment interaction: $F_{(1, 29)}$ = 10.43	**P <0.01	n=8-9 mice/genotype/treatment
Figure 2g	genotype: $F_{(1, 29)}$ = 14.64	***P <0.001	
Figure 2g	treatment: $F_{(1, 29)}$ = 26.30	***P <0.001	
Figure 2h	two-way ANOVA Bonferroni's multiple comparisons test; genotype x treatment interaction: $F_{(1, 24)}$ = 6.36	*P <0.05	n=7 mice/genotype/treatment
Figure 2h	genotype: $F_{(1, 24)}$ = 19.32	***P <0.001	
Figure 2h	treatment: $F_{(1, 24)}$ = 0.81	P = 0.38	
Figure 3b	two-way ANOVA Bonferroni's multiple comparisons test;	**P <0.01	n = 5/6 mice per group (average of n = 20 somas per slice, n = 2 slices per mouse, from

	genotype x treatment interaction: $F_{(1, 18)}$ = 9.35		three independent experiments)
Figure 3b	genotype: $F_{(1, 18)}$ = 4.09	*P <0.05	
Figure 3b	treatment: $F_{(1, 18)}$ = 30.95	***P <0.001	
Figure 4b	Mann-Whitney test WT Drd1- vs *Fmr1* KO Drd1-	P = 0.2898	n = 15 WT mice, n =14 *Fmr1* KO mice
Figure 4b	Mann-Whitney test WT Drd1+ vs *Fmr1* KO Drd1+	P = 0.3048	
Figure 4b	Mann-Whitney test *Fmr1* KO Drd1+ vs *Fmr1* KO Drd1-	P = 0.4013	
Figure 4c	Mann-Whitney test WT Drd1+ vs WT Drd1-	P = 0.0910	n = 15 WT mice, n =14 *Fmr1* KO mice
Figure 4c	Mann-Whitney test WT Drd1- vs *Fmr1* KO Drd1-	P = 0.4706	
Figure 4c	Mann-Whitney test WT Drd1+ vs *Fmr1* KO Drd1+	P = 0.0259	
Figure 4c	Mann-Whitney test *Fmr1* KO Drd1+ vs Fmr1 KO Drd1-	P = 0.0186	
Figure 4c	Mann-Whitney test *Fmr1* KO Drd1+ vs WT Drd1-	P = 0.041	
Figure 4d	Kolmogorov-Smirnov test *Fmr1* KO Drd1+ vs *Fmr1* KO Drd1-	P = 0.9206	n = 15 WT mice, n =14 *Fmr1* KO mice
Figure 4e	Kolmogorov-Smirnov test *Fmr1* KO Drd1+ vs *Fmr1* KO Drd1-	P <0.0001	n = 15 WT mice, n =14 *Fmr1* KO mice
Figure 4f	Mann-Whitney test	P <0.01	n = 9 mice/genotype (average of n = 3 slices per mouse)
Figure 4g	Mann-Whitney test	P = 0.162	n = 9 mice/genotype (average of n = 3 slices per mouse)
Figure 6b	two-way RM ANOVA Bonferroni's multiple comparisons test; time x genotype, $F_{(6,104)}$ = 4.44	***P <0.001	n=14 slices per group from 7 mice/genotype
Figure 6c	two-way ANOVA Bonferroni's multiple comparisons test; genotype x treatment interaction: $F_{(1, 39)}$ = 3.42	P = 0.07	n=10-11 mice/genotype/treatment
Figure 6c	genotype: $F_{(1, 39)}$ = 4.96	*P <0.05	
Figure 6c	treatment: $F_{(1, 39)}$ = 12.34	**P <0.01	
Figure 6d	two-way ANOVA Bonferroni's multiple comparisons test; genotype x treatment interaction: $F_{(1, 32)}$ = 4.67	*P <0.05	n=9 mice/genotype/treatment
Figure 6d	genotype: $F_{(1, 32)}$ = 19.31	***P <0.001	
Figure 6d	treatment: $F_{(1, 32)}$ = 2.79	P = 0.10	
Figure 6e	two-way ANOVA Bonferroni's multiple comparisons test;	*P <0.05	n=10 mice/genotype/treatment

	genotype x treatment interaction: $F_{(1, 36)}$ = 6.99		
Figure 6e	genotype: $F_{(1, 36)}$ = 11.10	**P <0.01	
Figure 6e	treatment: $F_{(1, 36)}$ = 0.62	P = 0.43	
Figure 7d	unpaired *t* test; $t_{(10)}$= 4.28	**P <0.01	n = 6 mice per group (average of n = 20 somas per slice, n = 2 slices per mouse, from three independent experiments
Figure 7e	unpaired *t* test; $t_{(17)}$= 3.40	**P <0.01	n=9-10 mice/genotype
Figure 7f	unpaired *t* test; $t_{(17)}$= 2.90	**P <0.01	n=9-10 mice/genotype
Figure 7g	unpaired *t* test; $t_{(17)}$= 2.38	*P <0.05	n=9-10 mice/genotype
Figure 7h	unpaired *t* test; $t_{(17)}$= 1.92	P =0.072	n=9-10 mice/genotype
Figure 7i	unpaired *t* test; $t_{(17)}$= 0.91	P =0.37	n=9-10 mice/genotype
Figure 7j	unpaired *t* test; $t_{(19)}$= 0.75	P =0.47	n= 10-11 mice/genotype
Figure 7k	unpaired *t* test; $t_{(17)}$= 2.80	*P <0.05	n=9-10 mice/genotype
Figure 7l	unpaired *t* test; $t_{(17)}$= 3.69	**P <0.01	n=9-10 mice/genotype

Table S1. Details of statistical tests.

Statistical details for all tests performed and information about the N for each experiment in main figures.